Insights into soft-part preservation from the Early Ordovician Fezouata Biota

Farid Saleh[1,2,3*], Romain Vaucher[4], Jonathan B. Antcliffe[5], Allison C. Daley[5], Khadija El Hariri[6], Khaoula Kouraiss[6], Bertrand Lefebvre[3], Emmanuel L.O. Martin[3], Jean Philippe Perrillat[3], Pierre Sansjofre[7], Muriel Vidal[8] & Bernard Pittet[3]

[1]*Yunnan Key Laboratory for Palaeobiology, Institute of Palaeontology, Yunnan University, Kunming, China*

[2]*MEC International Joint Laboratory for Palaeobiology and Palaeoenvironment, Institute of Palaeontology, Yunnan University, Kunming, China*

[3] *Université de Lyon, Université Claude Bernard Lyon 1, École Normale Supérieure de Lyon, CNRS, UMR5276, LGL-TPE, Villeurbanne, France*

[4] *Applied Research in Ichnology and Sedimentology (ARISE) Group, Department of Earth Sciences, Simon Fraser University, Burnaby, British Columbia V5A 1S6, Canada*

[5] *Institute of Earth Sciences, University of Lausanne, Géopolis, CH-1015 Lausanne, Switzerland*

[6] *Laboratoire de Géosciences et Environnement, Faculté des Sciences et Techniques, Université Cadi-Ayyad, BP 549, 40000 Marrakesh, Morocco*

[7] *MNHN, Sorbonne Université, CNRS UMR 7590, IRD, Institut de Minéralogie, Physique des Matériaux et de Cosmochimie, Paris, France*

[8] *Univ. Brest, CNRS, IUEM Institut Universitaire Européen de la Mer, UMR 6538 Laboratoire Géosciences Océan, Place Nicolas Copernic, 29280, Plouzané, France*

Corresponding author: Farid Saleh (farid.nassim.saleh@gmail.com)

Abstract

The Fezouata Biota in Morocco is the only Lower Ordovician Lagerstätte yielding a biologically diverse assemblage in a fully marine environment, whilst also containing organisms typical of Cambrian Burgess Shale-type (BST) ecosystems. Fossils from the Fezouata Shale share the same mode of preservation as Cambrian BST biotas defined by carbonaceous compressions and accessory authigenic mineralization. Most organisms of the Fezouata Biota were already dead and decaying on the seafloor when they were buried *in-situ* by occasional storm-induced deposits in an environment just below the storm-weather wave base. Pre-burial decay in the Fezouata Shale was responsible for the non-preservation of completely cellular organisms such as jellyfish. These conditions contrast with the processes described for soft-tissue preservation in the Burgess Shale (Canada) and the Chengjiang Biota (China). In these two Cambrian Lagerstätten, animals were transported alive or shortly after death by obrution events to an environment that was favorable for preservation. Despite preservational biases, the autochthonous assemblages of the Fezouata Shale offer a unique opportunity to decipher the structure of in-situ communities and ecological dynamics in Early Palaeozoic seas, when compared to the allochthonous communities of most Cambrian BST biotas.

Keywords: exceptional preservation, Cambrian, Fezouata Shale, Burgess Shale, Chengjiang Biota, taphonomy

1. Introduction

Fossils are key elements in deciphering ancient life on Earth. Much of our knowledge on biodiversification and extinction events comes from mineralized parts such as bones and shells because these are relatively abundant and are commonly found around the globe (Fan et al., 2020). However, organisms having mineralized parts constituting at least part of their bodies are not the sole components in modern ecosystems. A large number of animals are completely soft, having either cuticularized body walls (i.e. formed of polysaccharides), such as annelids and priapulids, or even entirely cellular bodies, such as jellyfish (e.g. Liu et al., 2008; Zhang et al., 2008; Lamsdell et al., 2013; Duan et al., 2014; Lei et al., 2014; Gutiérrez-Marco and García-Bellido, 2015; Martin et al., 2016a; Lerosey-Aubril et al., 2017). Thus, studies based on mineralized parts in the fossil record provide incomplete samples of past animal life on Earth. For this reason, incorporating information from localities with exceptional fossil preservation yielding labile anatomies is crucial to reconstruct ancient ecosystems more accurately (Daley et al., 2018). Although generally rare over the geological time scale, exceptionally preserved biotas discovered in deposits called "Lagerstätten" are common in the Cambrian (Gaines, 2014). The most famous Cambrian site with exceptional preservation is the Burgess Shale (Miaolingian, Canada; Butterfield 1990, 1995; Conway Morris, 1992; Gaines, 2014). The discovery of soft animal taxa in this locality transformed palaeontological knowledge on the earliest eumetazoan-dominated communities during the Cambrian Explosion (e.g. Daley et al., 2009, 2018; Smith and Caron, 2010; Moysiuk et al., 2017; Moysiuk and Caron, 2019; Nanglu et al., 2020). In the last 40 years, over 50 Burgess Shale-type (BST) assemblages have been discovered, most of them from the early to middle Cambrian (Gaines, 2014). Fossils from the Chengjiang Biota (Cambrian Series 2, China) preserved tissues that decay fast in laboratory conditions, and shed light on the early evolution of numerous metazoan phyla (Hou et al., 2004). For instance, nervous tissues were discovered in different arthropod groups ending long-

69 standing debates on the systematic affinities of these taxa (Ma et al., 2012, 2015; Tanaka et al.,
70 2013; Cong et al., 2014). The Chengjiang Biota yielded also the best fossilized cardiovascular
71 system ever discovered (Ma et al., 2014). All these animals from Cambrian BST assemblages
72 were preserved under similar environmental conditions and share the same mode of
73 preservation (Gaines et al., 2008, 2012a). They were transported from their living environment,
74 alive or shortly after their death by obrution events, to another setting, where they were buried
75 and eventually preserved (Gaines, 2014). The rapid transport and burial of these animals
76 provided a very limited time for oxic decay to occur, and increased the chances of tissues to
77 escape oxygen in the water column of their original environment (Gaines, 2014). In the deeper
78 facies where they were buried, anoxia was permissive at least at the sea bottom, and carbonate
79 cement precipitated on top of burial event deposits blocking exchange between the water
80 column and sediments and inhibiting oxidants from attaining decaying carcasses (Gaines et al.,
81 2012a). It was also recently suggested that specific clay minerals may have helped BST
82 preservation by slowing down bacterial decay (McMahon et al., 2016). Thus, carcasses were
83 isolated in a fine-grained lithology allowing their preservation in minute details as
84 carbonaceous compressions (Gaines et al., 2008). In some cases, authigenic mineralization (i.e.
85 pyritization, phosphatization) may have occurred, but this remained accessory to the primary
86 carbonaceous mode of preservation (Gaines et al., 2008). Then, for some sites (i.e. the Burgess
87 Shale, and Sirius Passet), the compressed organic matter was kerogenized and matured under
88 metamorphic conditions at temperatures between 300 and 400 degrees (Topper et al., 2018).
89 Although the general conditions for exceptional fossil preservation are relatively well-known
90 for Cambrian Lagerstätten, the mechanisms at play for soft-tissue preservation in younger BST
91 deposits remain largely unexplored.
92 In the early 2000s, a new Lagerstätte was discovered in the Zagora area, Central Anti-Atlas of
93 Morocco. The Fezouata Shale is, so far, the only unit to yield a highly diverse, fully marine

exceptionally preserved Ordovician biota (Van Roy et al., 2010, 2015a; Lefebvre et al., 2016a; Martin et al., 2016a). With more than 185 taxa of marine invertebrates recovered from numerous sites in the Zagora area, this formation offers new insights into the diversification of metazoans, at a key interval between the Cambrian Explosion and the Ordovician Radiation (Van Roy et al., 2010, 2015a; Lefebvre et al., 2016a). Most of these taxa are shelly organisms typical of the Ordovician Radiation including asterozoans, bivalves, rhynchonelliformean brachiopods, cephalopods, crinoids, gastropods, graptolites, ostracods, and trilobites (Fig. 1). The Fezouata Biota also comprises a high number of soft-bodied to lightly sclerotized taxa (Fig. 1). Some of these exceptionally preserved organisms (e.g. cirriped crustaceans, eurypterid and xiphosuran chelicerates) represent the oldest occurrences of important marine invertebrate groups, previously only recorded from younger Lagerstätten (Van Roy et al., 2015a). The Fezouata Biota also includes abundant representatives of taxa typical of Cambrian age BST Lagerstätten (e.g. radiodonts, protomonaxonids, armored lobopodians, marrellomorphs, naraoiids) (Botting, 2007, 2016; Vinther et al., 2008, 2017; Van Roy et al., 2010, 2015b; Pérez-Peris et al., in press).

Two modes of exceptional preservation have been documented in the Fezouata Shale. The first one occurs in concretions (Gaines et al., 2012b). The second type of exceptional preservation is associated with shales in a generally shallower environment in comparison to the classical Burgess Shale (Martin et al., 2016a; Vaucher et al., 2016). Most Fezouata BST fossils collected in shales are preserved as molds or imprints on the sediments (Martin et al., 2016a), and it is unclear whether these organisms were originally preserved as carbonaceous compressions. In some cases, some non-biomineralized tissues in flattened fossils, such as trilobite digestive tracts and echinoderm water-vascular systems, are preserved in 3D iron oxides (Van Roy et al., 2010; Gutiérrez-Marco et al., 2017; Lefebvre et al., 2019).

Considering that numerous mechanisms may favor or alter the preservation of original anatomies in fossils (Fig. 2), deciphering the taphonomic processes is essential for palaeontological and ecological studies, especially for taxa without extant representatives. Consequently, the aim of this study is to review soft tissue taphonomy in the Fezouata Shale based on a multidisciplinary approach combining data across palaeontology, sedimentology, geochemistry and mineralogy. This in-depth reconstruction starts at the life of an organism in its environment and ends at its discovery in surface sediments passing through biostratinomy, diagenesis, metamorphism, and modern weathering (Fig. 2) (Sansom et al., 2010; Bath Enright, 2018; Parry et al., 2018; Purnell et al., 2018). To do so, we will answer the five following questions:

- Question 1: What is the stratigraphic distribution of exceptional preservation in the Fezouata Shale?
- Question 2: What were the sedimentary surface processes affecting organisms?
- Question 3: Under what conditions did decay and diagenetic mineralization take place?
- Question 4: What were the post-diagenetic processes?
- Question 5: What is the fidelity of preservation in the Fezouata Shale?

Answering these questions allows for comparison of the Fezouata Shale communities and their preservation with both the Burgess Shale and the Chengjiang Biota. This comparison is essential to constrain preservation biases within exceptionally preserved biotas and thus to reconstruct early animal ecosystem evolution. This work has implications in understanding the earliest radiations of complex metazoans on Earth from a fresh perspective that accounts for individual preservation biases that were likely operational at each site.

2. Question 1: stratigraphic context – discontinuous occurrences of exceptional preservation

143 The Fezouata Shale is largely exposed in the Anti-Atlas of Morocco. During the Early
144 Ordovician, this area was located at high latitudes close to the palaeo-South pole (Torsvik and
145 Cocks, 2011, 2013). In the Anti-Atlas, the Ordovician succession (maximum ~2500m thick to
146 the West) was originally divided into four lithostratigraphic groups, which are in stratigraphic
147 order: the Outer Feijas, the First Bani, the Ktaoua, and the Second Bani (Fig. 3) (Choubert,
148 1942). Following the stratigraphic work of Destombes in the second half of the 20th century,
149 these stratigraphic groups were subdivided into several formations (Fig. 3) (Destombes, 1970,
150 1971; Destombes et al., 1985). The Fezouata Shale (Tremadocian–Floian) is unconformably
151 deposited over the middle Cambrian Tabanite Group and is conformably overlained by the Zini
152 Formation (late Floian) that is itself overlain by the Tachilla Formation (Darriwilian) (Fig. 3)
153 (Destombes, 1970, 1971; Destombes et al., 1985). The Fezouata Shale is a siltstone-dominated
154 formation outcropping in an area of 900 km^2 in the Zagora region and with a total thickness of
155 ~ 900 m (Martin et al., 2016b, Vaucher et al., 2016) with sandstone layers becoming more
156 common in the upper part of the formation (Vaucher et al., 2016, 2017). Although mineralized
157 fossils were discovered since the early excavations in the first half of the 20th century,
158 exceptional fossil preservation in the Fezouata Shale was not documented until the early years
159 of the 21st century (Van Roy et al., 2010; Lefebvre et al., 2016a). In the Fezouata Shale, the
160 distribution of exceptional preservation is not random. Exceptionally preserved fossils are
161 found in two distinct stratigraphic intervals (Lefebvre et al., 2016a, 2018). Based on acritarchs,
162 conodonts, and graptolites (Gutiérrez-Marco and Martin, 2016; Lehnert et al., 2016; Nowak et
163 al., 2016; Lefebvre et al., 2018), a late Tremadocian age (Tr3) was proposed for the lower,
164 about 70-m thick interval (*A. murrayi* graptolite biozone; Fig. 3). The upper interval is thinner
165 (~50-m thick), and it occurs about 240 m higher in the succession (Lefebvre et al., 2018).
166 Graptolites suggest a mid-Floian age (Fl2) for this upper interval (Fig. 3) (Gutiérrez-Marco and
167 Martin, 2016; Lefebvre et al., 2018). This review focuses on exceptionally preserved material

168 from the lower interval, because it is stratigraphically well constrained (Van Roy et al., 2010;
169 Martin et al., 2016a; Lefebvre et al., 2018). Within this interval, soft-parts are not found
170 everywhere (Saleh et al., 2019). They occur in discontinuous levels with a periodicity of
171 100,000 years pointing to a possible eccentricity control through seasonality on this type of
172 preservation (Fig. 3) (Saleh et al., 2019). The control of eccentricity on seasonality (Fig. 3)
173 suggests that the conditions favoring this type of preservation were more likely to be ephemeral
174 than permanent (Saleh et al., 2019).
175
176 **3. Question 2: surface processes – *in-situ* burial by distal tempestites**
177 The lithology of the Fezouata Shale varies from claystone to fine-grained sandstone (Vaucher
178 et al., 2016, 2017; Saleh et al., 2020a), while most of the sedimentary succession of this
179 formation is constituted of siltstones (Vaucher et al., 2016, 2017; Saleh et al., 2020a). The
180 sedimentary structures found in the Fezouata Shale are typical of a storm-wave dominated
181 environment (Fig. 4A) (Martin et al., 2016; Vaucher et al., 2016, 2017; Saleh et al., 2020a).
182 These storms were erosive, and their deposits are characterized by the presence of normally
183 graded beds (Fig. 4A, C) (Saleh et al., 2020a), and by oscillatory ripples that were increasing
184 in wavelength from distal (null to millimetric wavelength) to proximal settings (metric to
185 plurimetric wavelength) (Fig. 4B, D) (Vaucher et al., 2016, 2017). Storm-wave deposits are
186 discontinuous in the Fezouata Shale. In proximal settings, a tidal modulation of storm waves
187 occurred and is recorded as a repeated stack of larger (low tide) to smaller (high tide) oscillatory
188 structures within fine-grained sandstones (Fig. 4E) (Vaucher et al., 2017). A statistical
189 correlation between sedimentological data from cores and palaeontological data from outcrops
190 showed that exceptional preservation is associated with one of the most distal facies of the
191 Fezouata Shale (Fig. 5) (Saleh et al., 2020a). This facies is characterized with an abundance of
192 mudstones (i.e. an average of 60% illite $\{(K,H_3O)(Al,Mg,Fe)_2(Si,Al)_4O_{10}[(OH)_2,(H_2O)]\}$, 10%

193 of various chlorite minerals, and 30% siltstones (quartz SiO_2) (Saleh et al., 2019). In this facies,
194 event deposits are not stacked and are separated by background sediments (Saleh et al., 2020a).
195 Furthermore, oscillatory structures are absent indicating that these sediments represent storm-
196 induced deposits in an environment just below the storm wave base (SWB; Fig. 5).
197 Furthermore, exceptionally preserved fossils in this facies are interpreted as autochthonous,
198 because they are occurring right under and not within burial deposits (Fig. 4F, G) (Vaucher et
199 al., 2016; Saleh et al., 2018; 2020a,b). When fossils are disarticulated, this results from in-situ
200 decay rather than transportation, because they do not show any preferential orientation (Fig.
201 4F) with little evidence of physical abrasion (Martin et al., 2015; Lefebvre et al., 2016a; Saleh
202 et al., 2018; Vannier et al., 2019). In fact, only strong storms are accountable for the
203 accumulation of very coarse siltstones to very fine sandstones in this setting causing an
204 entombment delay and the decay of dead organisms on the seafloor (Saleh et al., 2020a). Due
205 to this pre-burial decay, many fossiliferous intervals yielded hundreds of fossils from which
206 only tens preserved soft-structures (Lefebvre et al., 2019; Saleh et al., 2020a). The rarity of
207 storm-induced deposits in distal settings and its impact on living communities in the Fezouata
208 Shale is validated through observations on body-size fluctuations between sites of this
209 formation (Saleh et al., 2018; 2020b). In proximal sites, sessile epibenthic organisms were
210 recurrently buried by storm deposits and could not attain large sizes (Fig. 5). On the contrary
211 nearshore endobenthic taxa were not affected by these events and, if sufficiently motile, they
212 could survive and reach larger sizes (Fig. 5) (Saleh et al., 2018). It was also evidenced that
213 vagile benthic trilobite taxa, distributed in all fossiliferous environments of the Fezouata Shale,
214 reached larger size in distal settings of this formation due to minimal physical stress in distal
215 environments (Fig. 5) (Saleh et al., 2020b). Some of them possibly migrated during storm
216 seasons from proximal to distal settings (Vannier et al., 2019). However, an increase in body-
217 size for epibenthic taxa from proximal to distal sites of the Fezouata Shale should not be

generalized. Specific levels in intermediate settings of this formation are characterized by low diversity assemblages with an abundance of small-sized individuals (Fig. 5) (Martin, 2016; Martin et al., 2016b). This possibly indicates that oxygenation was not stable and periods with lower oxygen concentration existed in these settings, suggesting a temporary or seasonal oxygen minimum zone (OMZ)-like conditions (Fig. 5). This hypothesis needs further testing using a geochemical approach.

4. Question 3: early diagenesis – controlled decay and authigenic mineralization

In the Fezouata Shale there must be some conditions controlling pre-burial decay and compensating for the delay in fossil entombment for exceptional preservation to occur. Pre-burial decay in the Fezouata Shale was controlled and slowed down by a favorable clay mineralogy (Saleh et al., 2019). Chamosite (i.e. originally berthierine) (Fig. 6C) appears to be present in all analyzed levels recording exceptional preservation (i.e. 6 in total), and absent from intervals with skeletal preservation (i.e. 7 levels) (Saleh et al., 2019). Both berthierine and its primary precursor (Anderson et al., 2018) have been shown to slow down decay under experimental conditions with open oxygenic atmospheric diffusion by damaging bacterial cells (McMahon et al., 2016). This may be the main factor that helped some labile anatomies survive delays in entombment by storm-induced deposits in distal facies (Saleh et al., 2019).

When burial occurs, and if it leads to the establishment of anoxic conditions, another type of decay takes place (Fig. 2). Anoxic decay transforms organic matter from decaying carcasses with sulfates SO_4^{2-} from seawater into sulfides H_2S. SO_4^{2-} is not a limiting parameter for this reaction in marine environments. Thus, the H_2S output is mainly controlled by the decay products of biological tissues. High quantities of available organic material such as in the cases of giant decaying arthropods (e.g. 2 meters long *Aegirocassis* radiodonts) leads to the establishment of prominent chemical gradients around carcasses and to the early precipitation

and mineral overgrowth around tissues, resulting in their preservation in concretions (Gaines et al., 2012b). However, normal-sized individuals produce less H_2S leading to a less prominent chemical gradient that is not capable of initializing concretion growth (Gaines et al., 2012b). Nevertheless, H_2S can still react with iron from the sediments to form pyrite crystals under anoxic conditions (Raiswell et al., 1993; Schiffbauer et al., 2014). The establishment of anoxic conditions at the time of burial, and H_2S production in the Fezouata Shale lead to the precipitation of framboid and small euhedral crystals in fossils as well as fresh pyrite in non-altered sediments (Fig. 6) (Saleh et al., 2020a). In these sediments, C is also associated with pyrite, possibly suggesting that the original mode of preservation in the Fezouata Shale was comparable to that of the Burgess Shale and the Chengjiang Biota comprising both organic material and authigenic minerals (Gaines et al., 2008; Saleh et al., 2020a,c). As no fossil shows complete pyritization and pyrite precipitation remains rare and tissue-selective, other parameters were also likely controlling pyrite precipitation in the Fezouata Shale (Saleh et al., 2020c). For instance, cuticles of many arthropod taxa are preserved without any pyrite crystals. This can result from H_2S limitation considering that this structure is formed of polysaccharides that are not easily degradable (i.e. quantity of decayed organic matter is not enough to reduce SO_4^{2-}) (Gabbott et al., 2004). However, when comparing internal labile tissues to each other, the model based on H_2S limitation cannot explain why some tissues are pyritized, while others decayed and disappeared (meaning they reduced SO_4^{2-}) without pyritizing (Saleh et al., 2020c). The clue probably lies in Fe availability. Maghemite is found associated with pyrite in some analyzed samples under Raman Spectroscopy (Fig. 6) (Saleh et al., 2020c). Maghemite results from the burial of an original mineral called ferrihydrite $[FeO(OH)]_8[FeO(H_2PO_4)]$ (Mazzetti and Thistlethwaite, 2002). Ferrihydrite is a widely distributed biological mineral (Aldred et al., 2009; Hoda et al., 2013; Dunaief et al., 2014). Under anoxic and sulfated conditions, ferrihydrites release high quantities (~ 87%) of reactive Fe (Li et al., 2006) very fast (i.e. half-

life of only 2.8 hours) (Canfield et al., 1992). This is 100 times faster than goethite, 270 times faster than hematite and 2000 times faster than reactive silicates (Canfield et al., 1992). For this reason, in order to understand the patterns of exceptional preservation in the Fezouata Shale, but also in Lagerstätten such as Chengjiang and the Beecher's Trilobite Bed in which pyrite played a role in preserving decay-prone anatomies, three parameters should be taken into account: Fe in sediments, Fe in labile tissues, and H_2S production (Saleh et al., 2020c). Accounting for both pre-burial and anoxic decay, different scenarios emerge and are summarized in Fig. 6.

- In the first scenario, pre-burial decay is not restricted by any mineralogical phase and burial allowing the establishment of anoxic conditions is delayed. Pyritization does not occur rapidly enough, leaving only body walls (e.g. trilobite carapaces) preserved (Fig. 6A).
- In the second scenario, burial occurs establishing anoxic conditions for pyritization. Fe in burial material is highly reactive leading to the complete pyritization of the organism, if it is buried alive (Fig. 6B). If the animal decayed on the seafloor but the activity of its degradation was controlled by clay/chlorite minerals, the reactivity of Fe from sediments ensures the pyritization of all tissues that survived pre-burial decay (Fig. 6C). Due to extreme iron reactivity, even carapaces of numerous arthropod taxa that provide small quantities of H_2S are found pyritized in sites such as the Beecher's Trilobite Bed (Briggs et al., 1991; Raiswell et al., 1993, 2008).
- In the third scenario, pre-burial decay is controlled by clay/chlorite minerals. However, after burial, a delay in iron availability in the sediment allows the disappearance of tissues owing to anaerobic decay. The least labile internal tissues will potentially survive anoxic decay and get pyritized once iron from sediments becomes available (Fig. 6D). This scenario explains the selective preservation of guts, while more labile tissues (e.g. nervous systems) are absent (Gutiérrez-Marco et al., 2017).

- In the fourth scenario, pre-burial decay does not occur at all as if animals were buried alive. However, Fe in this scenario is not reactive (even if it is abundant). Thus, only tissues that are rich originally in iron will get preserved and pyritized, even if they are the most labile ones (Fig. 6E). This scenario can explain the preservation of extremely decay-prone structures such as nervous tissues as pyrite replicates in fossils from the Chengjiang Biota (Ma et al., 2012, 2015; Tanaka et al., 2013; Cong et al., 2014).

Considering the decay stages of animals from the Fezouata Shale, the lower availability of iron in sediments in this formation in comparison to sites such as Beecher's Trilobite Bed, and the absence of preserved nervous systems comparable to those occurring in Chengjiang, it is most probable that the taphonomic scenario of most exceptionally preserved fossils found in the Fezouata Shale followed the third scenario (Fig. 6D). However, this pathway is not exclusive, and other scenarios may have accounted for the discovery of only biomineralized parts in some levels from this formation (Fig. 6A). Furthermore, there might have been other parameters facilitating exceptional preservation in the Fezouata Shale. The dominance of storm-induced deposits, the presence of a favorable clay mineralogy and the selective authigenic mineralization surely helped exceptional preservation to occur in this formation. However, these conditions can be acquired in a wide range of marine settings while Ordovician exceptionally preserved biotas remain scarce. The position of the Fezouata Shale near the South pole in a generally cold water environment might have favored the occurrence of exceptional fossil preservation by slowing down decay rates.

5. Question 4: post-diagenesis – minimal maturation and extensive modern weathering

Raman spectroscopy-based models for thermal maturation on carbon indicate that the Fezouata Shale sediments were buried at maximum temperatures of 200°C (Rahl et al., 2005; Kouketsu et al., 2014; Saleh et al., 2019, 2020a). Thus, metamorphism *sensu stricto* and organic remain

318 volatilization (Fig. 2) did not occur (Saleh et al., 2019, 2020a). In the absence of metamorphism,
319 calcium leaching and the enrichment of manganese in fossils (e.g. Ca leaching from the skeletal
320 elements of solutan echinoderms and the Mn enrichment around the appendages of
321 marrellomorph arthropods (Fig. 7) in the Fezouata Shale are most probably due to modern
322 weathering (Fig. 2). In the Draa Valley, this formation is exposed to abundant water circulation
323 (Warner et al., 2013). Outcrops are surrounded by abandoned terraces and by numerous water
324 wells (Warner et al., 2013). Circulating waters in arid environments with occasional rain falls
325 similar to the Draa Valley are rich in manganese oxides that can start the oxidation of the tissues
326 that were selectively and three dimensionally preserved in pyrite during early diagenesis in
327 addition to the rest of the fossil (Fig. 7A) (Potter and Rossman, 1979; Warner et al., 2013). The
328 resulting products of this reaction are Fe-oxides in the shape of the original pyrite crystals (i.e.
329 euhedral or framboidal) and Mn-sulfates (Fig. 7B) (Larsen and Postma, 1997). If the quantities
330 of Mn are not sufficient to fully oxidize pyrite, pyrite oxidation can further continue through
331 the usage of dissolved oxygen in pore waters (Fig. 7B) and unleash considerable amounts of
332 sulfuric acid (Fig. 7C), thus reducing the pH of the environment and contributing to the
333 dissolution of nearby carbonates (Larsen and Postma, 1997) such as the skeletal elements of
334 echinoderms (Fig. 7D). When extensive weathering occurs by circulating waters that are Fe-
335 rich, C can be completely leached from flattened fossils and star-shaped iron oxides can be
336 deposited (Fig. 7E) (Saleh et al., 2020a). These star-shaped and modern iron oxides do not result
337 from pyrite oxidation (Fig. 7) (Saleh et al., 2020a) and they account for the red/orange color of
338 many flattened fossils found in the Fezouata Shale (Fig. 1). Although these minerals are
339 weathering products, they lead to an easier differentiation of biological features from the
340 surrounding sediments. This can be evidenced when comparing extensively weathered and less
341 altered fossils belonging to the same animal group such as marrellomorphs (Fig. 7).

6. Question 5: preservation fidelity – underestimation of completely cellular organisms

The Fezouata Shale is major step forward to complete our understanding of the taphonomic mechanisms behind BST preservation in addition to deciphering how these mechanisms influence the patterns of fossil preservation during the Palaeozoic. Burgess Shale-type animals in the Fezouata Biota are preserved just below the SWB. This contrasts with their preservation in much deeper settings during the Cambrian (e.g. the Burgess Shale, Qingjiang Biota) (Gaines, 2014; Fu et al., 2019), and indicates that BST preservation can occur under different bathymetries. Furthermore, the Fezouata Shale shows that BST preservation can occur even if carcasses were exposed on the seafloor prior to their burial as some clay minerals with antibacterial properties can reduce the impact of oxic decay (McMahon et al., 2016; Anderson et al., 2018, 2020a; Saleh et al., 2019). However, this facilitating condition is not enough on its own for soft-structures to preserve because these clay minerals do not stop aerobic bacterial decay; they simply slow it down (McMahon et al., 2016). Most importantly, even if a certain tissue survived oxic degradation it can still decay after burial when different redox conditions and new bacterial communities take over the degradation process (Fig. 6D, E) (Hancy and Antcliffe, 2020). This post-burial degradation can be mitigated by authigenic mineralization such as pyrite or phosphate precipitation (Saleh et al., 2020c; Gueriau et al., 2020) or even by the association of clay minerals such as kaolinite to certain labile anatomies (Anderson et al. 2020b). Authigenic pyritization happens when iron is available and anoxic conditions are established in sediments, but oxidants from the water column (i.e. sulfates) can still reach decaying carcasses (Raiswell et al., 1993, Saleh et al., 2020c). Carbonate cement, found in many Cambrian Lagerstätten, capping event deposits and blocking oxidants from attaining decaying carcasses, are absent from all sediments in the Fezouata Shale which can explain why pyritization is more abundant in this site than in the Walcott Quarry (Burgess Shale) for

example (Saleh et al., 2020a). The last main difference between the Fezouata Shale and most Cambrian Lagerstätten is that fossil transport was not operational at the Ordovician site (Martin et al., 2016a; Vaucher et al., 2016, 2017; Saleh et al., 2018, 2020a, b). All these aforementioned preservational discrepancies indicate that there is no single condition that can be considered as a pre-requisite for BST preservation. BST preservation is a trade-off between decay and mineralization (Fig. 6). This trade-off is controlled by interacting parameters (e.g. transport, oxygen, carbonate cement, specific clay minerals, bacteria). This interaction dictates what and how tissues get preserved in a certain site and the impact of this interaction on preservation can be easily investigated by comparing the co-occurrence of biological structures (Fig. 8A) in these deposits, because all animals are originally made of the same types of structures (e.g. mineralized, cuticularized, cellular, sclerotized) (Saleh et al., 2020d). It has been recently evidenced that biological structure association in the Fezouata Shale is significantly different from that at the Burgess Shale and the Chengjiang Biota (Saleh et al., 2020d). Most taxa in the Walcott Quarry and the Chengjiang Biota preserved two to three types of biological structures at the same time (e.g. cuticle and sclerites; or cuticle, sclerites, and cellular tissues, Fig. 8B) (Saleh et al., 2020d). Most taxa in the Fezouata Shale preserved one type of biological structures at a time (Fig. 8B) (Saleh et al., 2020d). Most importantly, the Fezouata Shale systematically failed to preserve soft cellular structures that are in direct contact with seawater in addition to completely cellular organisms. These results suggest that biodiversity is very likely underestimated in the Fezouata Biota (Fig. 8C) (Saleh et al., 2020d). The absence of these structures can be either linked to (1) the fact that cellular structures in direct contact with sea water (e.g. tentacles of hyoliths) are generally the most labile and the fastest to decay (even when clay minerals with antibacterial properties are present) and/or (2) the lack of required conditions for their mineralization (Saleh et al., 2020d). The magnitude of this underestimation can be quantitively assessed by looking at the proportion of entirely cellular taxa in Cambrian

Lagerstätten. In the Walcott Quarry and the Chengjiang Biota, entirely cellular organisms (e.g. chordate, medusoids) constitute 13 and 10% respectively of original animal communities in these sites (Saleh et al., 2020d). If the Fezouata Biota had a similar taxonomic composition to the Walcott Quarry and the Chengjiang Biota, the total diversity of this site is most probably underestimated by at least 10% (entirely cellular organisms being completely absent). Since this taphonomic bias can be identified and accounted for, the in-situ preservation in the Fezouata Shale becomes an asset for sophisticated ecological studies that examine the evolution of community structure during the Palaeozoic at the transition between the Cambrian Explosion and the Ordovician Radiation. Cambrian ecosystems contrast with Ordovician ones (niche vs dispersal assembled) (Na and Kiessling, 2015; Rasmussen et al., 2019; Stigall et al., 2019). The Fezouata Shale is the only exceptionally preserved biota with hundreds of fossiliferous levels within two stratigraphic intervals (Tremadocian and Floian in age), providing a database that can be used to describe the continuum of ecological change between major Palaeozoic evolutionary events and to decipher if the transition from niche to dispersal-built ecosystems was abrupt or gradual (Harper and Servais, 2018; Rasmussen et al., 2019; Servais et al., 2019; Stigall et al., 2019).

7. Conclusions

The Fezouata Shale constitutes a unique record of marine life in the Lower Ordovician. It contains two stratigraphic intervals bearing exceptionally preserved animals (Tremadocian and Floian in age), and documenting an unexpected evolutionary melting pot of Cambrian BST-like holdovers co-occurring with typical members of the Ordovician Radiation. These animals lived in a shallow marine environment that is dominated by storms and were exceptionally preserved *in-situ* just below the SWB. Due to the rarity of storm-induced deposits affecting distal settings, most soft parts decayed prior to their burial. This decay activity was slowed

down by a specific clay mineralogy. When favorable conditions for pyritization occurred after burial, pyrite precipitated in specific tissues. In the Fezouata Shale, fossils were originally preserved as carbonaceous compressions with accessory authigenic mineralization in a similar way to Cambrian BST deposits. However, modern water circulation within outcrops leached most of the organic carbon from fossils and oxidized pyrite. Even though the mode of preservation appears to be universal between both Cambrian and Ordovician BST deposits, our review highlights that there are some discrepancies in the mechanisms that lead to this type of preservation. The pre-burial decay in the Fezouata Shale largely contributed to the non-preservation of both soft cellular structures in direct contact with seawater and cellular organisms (e.g. chordates, jellyfish), thus leading to an underestimation of the original diversity of this biota. In spite of this underestimation, the Fezouata Shale is unique in providing an *in-situ*, fully marine community of Burgess Shale-type. The Fezouata Biota represents a series of highly diverse high-latitude communities, at the transition between the Cambrian Explosion and the Ordovician Radiation and as such sits at a critical crossroads in understanding the early evolution of complex animal communities.

Acknowledgments

This paper is supported by a grant of the Chinese Postdoctoral Science Foundation awarded to FS. This paper is also a contribution to the TelluS-Syster project 'Vers de nouvelles découvertes de gisements à préservation exceptionnelle dans l'Ordovicien du Maroc' (2017) and the TelluS-INTERRVIE projects 'Mécanismes de préservation exceptionnelle dans la Formation des Fezouata' (2018), and 'Géochimie d'un Lagerstätte de l'Ordovicien inférieur du Maroc' (2019) all funded by the INSU (Institut National des Sciences de l'Univers, France), CNRS. This paper is as well a contribution to the International Geoscience Programme (IGCP) Project 653 – The onset of the Great Ordovician Biodiversification Event. This paper is supported by Grant no.

205321_179084 from the Swiss National Science Foundation, awarded to ACD as Principal Investigator. The authors are particularly grateful to Yves Candela, Lukáš Laibl, Pierre Gueriau, Martina Nohejlovà, Eric Monceret, Stephen Pates, Daniel Vizcaïno, Francesc Pérez-Peris, and Lorenzo Lustri who helped in the field. Orla Bath Enright is thanked for fruitful discussions. Associate Editor Christopher Fielding and two anonymous reviewers are also thanked for their positive comments and insightful reviews.

References

Aldred, E.M., Buck, C., Vall, K., Aldred, E.M., Buck, C., Vall, K., 2009. Scientific tests. Pharmacology 331–341. https://doi.org/10.1016/B978-0-443-06898-0.00041-4

Anderson, R.P., Tosca, N.J., Gaines, R.R., Mongiardino Koch, N., Briggs, D.E.G., 2018. A mineralogical signature for Burgess Shale–type fossilization. Geology 46, 347–350. https://doi.org/10.1130/G39941.1

Anderson, R.P., Tosca, N.J., Cinque, G., Frogley, M.D., Lekkas, I., Akey, A., Hughes, G.M., Bergmann, K.D., Knoll, A.H. and Briggs, D.E.G, 2020a. Aluminosilicate haloes preserve complex life approximately 800 million years ago. Interface Focus, 10(4), 20200011.

Anderson, R.P., Tosca, N.J., Saupe, E.E., Wade, J., Briggs, D.E.G., in press. Early formation and taphonomic significance of kaolinite associated with Burgess Shale fossils. Geology. doi: https://doi.org/10.1130/G48067.1

Bath Enright, O.G., 2018. Investigating the impacts of transport and decay on the polychaete *Alitta Virens*: Implications for the taphonomy of the Burgess Shale. Unpubl. PhD thesis, University of Portsmouth. p. 305.

Botting, J.P., 2007. 'Cambrian' demosponges in the Ordovician of Morocco: insights into the early evolutionary history of sponges. Geobios 40, 737–748.

Botting, J.P., 2016. Diversity and ecology of sponges in the Early Ordovician Fezouata Biota,

Morocco. Palaeogeogr. Palaeoclimatol. Palaeoecol. 460, 75–86.

Briggs, D.E., Bottrell, S.H., and Raiswell, R., 1991. Pyritization of soft-bodied fossils: Beecher's trilobite bed, Upper Ordovician, New York State. Geology 19(12), 1221–1224.

Butterfield, N.J., 1990. Organic preservation of non-mineralizing organisms and the taphonomy of the Burgess Shale. Paleobiology 16(3), 272-286.

Butterfield, N.J., 1995. Secular distribution of Burgess-Shale-type preservation. Lethaia, 28(1), 1-13.

Canfield, D.E., Raiswell, R., Bottrell, S., 1992. The reactivity of sedimentary iron minerals toward sulfide. Am. J. Sci. 292, 659–683. https://doi.org/10.2475/ajs.292.9.659

Choubert, G., 1942. Constitution et puissance de la série primaire de l'Anti-Atlas. C. R. Acad. Sci. Paris 215, 445-447.

Cong, P., Ma, X., Hou, X., Edgecombe, G.D., Strausfeld, N.J., 2014. Brain structure resolves the segmental affinity of anomalocaridid appendages. Nature 513, 538–542. https://doi.org/10.1038/nature13486

Conway Morris, S., 1992. Burgess Shale-type faunas in the context of the 'Cambrian explosion': a review. Journal of the Geological Society 149(4), 631-636.

Daley, A.C., Budd, G.E., Caron, J.B., Edgecombe, G.D., Collins, D., 2009. The Burgess Shale anomalocaridid *Hurdia* and its significance for early euarthropod evolution. Science 323, 1597–1600.

Daley, A.C., Antcliffe, J.B., Drage, H.B., Pates, S., 2018. Early fossil record of Euarthropoda and the Cambrian Explosion. Proc. Natl. Acad. Sci. 115, 5323–5331. https://doi.org/10.1073/PNAS.1719962115

Destombes, J., 1970. Cambrien et Ordovicien. Notes et Mém. Serv. géol. Maroc 229, 161-170.

492 Destombes, J., 1971. L'Ordovicien au Maroc. Essai de synthèse stratigraphique. Mém. Bur.
493 Rech. Géol. Min. 73, 237-263.
494 Destombes, J., Hollard, H., Willefert, S., 1985. Lower Palaeozoic rocks of Morocco, in:
495 Holland, C. (Ed.), Lower Palaeozoic Rocks of the World. John Wiley and Sons,
496 Chichester, pp. 91–336.
497 Duan, Y., Han, J., Fu, D., Zhang, X., Yang, X., Komiya, T., Shu, D., 2014. Reproductive
498 strategy of the bradoriid arthropod *Kunmingella douvillei* from the Lower Cambrian
499 Chengjiang Lagerstätte, South China. Gondwana Res. 25, 983–990.
500 https://doi.org/10.1016/J.GR.2013.03.011
501 Dunaief, D., Cwanger, A., Dunaief, J.L., 2014. Iron-Induced Retinal Damage. Handb. Nutr.
502 Diet Eye 619–626. https://doi.org/10.1016/B978-0-12-401717-7.00063-0
503 Fan, J.X., Shen, S.Z., Erwin, D.H., Sadler, P.M., MacLeod, N., Cheng, Q.M., Hou, X.D.,
504 Yang, J., Wang, X.D., Wang, Y., Zhang, H., Chen, X., Li, G.X., Zhang, Y.C., Shi, Y.K.,
505 Yuan, D.X., Chen, Q., Zhang, L.N., Li, C., Zhao, Y.Y., 2020. A high-resolution
506 summary of Cambrian to early Triassic marine invertebrate biodiversity. Science 367,
507 272–277. https://doi.org/10.1126/science.aax4953
508 Farrell, U.C., Briggs, D.E.G., Gaines, R.R., 2011. Paleoecology of the olenid trilobite
509 *Triarthurus*: new evidence from Beecher's Trilobite Bed and other sites of pyritization.
510 Palaios 26, 730–742. https://doi.org/10.2110/palo.2011.p11-050
511 Fu, D., Tong, G., Dai, T., Liu, W., Yang, Y., Zhang, Y., Cui, L., Li, L., Yun, H., Wu, Y. and
512 Sun, A., 2019. The Qingjiang biota: a Burgess Shale-type fossil Lagerstätte from the
513 early Cambrian of South China. Science 363(6433), pp.1338-1342.
514 Gabbott, S.E., Xian-guang, H., Norry, M.J., Siveter, D.J., 2004. Preservation of Early
515 Cambrian animals of the Chengjiang Biota. Geology 32, 901.
516 https://doi.org/10.1130/G20640.1

517 Gaines, R.R., 2014. Burgess Shale-type preservation and its distribution in space and time.
518 Paleontol. Soc. Pap. 20, 123–146. https://doi.org/10.1017/S1089332600002837
519 Gaines, R.R., Briggs, D.E.G., Yuanlong, Z., 2008. Cambrian Burgess Shale–type deposits
520 share a common mode of fossilization. Geology 36, 755.
521 https://doi.org/10.1130/G24961A.1
522 Gaines, R.R., Hammarlund, E.U., Hou, X., Qi, C., Gabbott, S.E., Zhao, Y., Peng, J., Canfield,
523 D.E., 2012a. Mechanism for Burgess Shale-type preservation. Proc. Natl. Acad. Sci. U.
524 S. A. 109, 5180–4. https://doi.org/10.1073/pnas.1111784109
525 Gaines, R. R., Briggs, D.E.G., Orr, P.J., Van Roy, P., 2012b. Preservation of giant
526 anomalocaridids in silica-chlorite concretions from the Early Ordovician of Morocco.
527 Palaios 27, 317–325. https://doi.org/10.2110/palo.2011.p11-093r
528 Gueriau, P., Bernard, S., Farges, F., Mocuta, C., Dutheil, D.B., Adatte, T., Bomou, B., Godet,
529 M., Thiaudière, D., Charbonnier, S. and Bertrand, L., 2020. Oxidative conditions can
530 lead to exceptional preservation through phosphatization. Geology.
531 Gutiérrez-Marco, J.C., García-Bellido, D.C., 2015. Micrometric detail in palaeoscolecid
532 worms from Late Ordovician sandstones of the Tafilalt Konservat-Lagerstätte, Morocco.
533 Gondwana Res. 28, 875–881. https://doi.org/10.1016/J.GR.2014.04.006
534 Gutiérrez-Marco, J.C., García-bellido, D.C., Rábano, I., Sá, A.A., 2017. Digestive and
535 appendicular soft-parts, with behavioural implications, in a large Ordovician trilobite
536 from the Fezouata. Sci. Rep. 7, 1–7. https://doi.org/10.1038/srep39728
537 Gutiérrez-Marco, J.C., Martin, E.L.O., 2016. Biostratigraphy and palaeoecology of Lower
538 Ordovician graptolites from the Fezouata Shale (Moroccan Anti-Atlas). Palaeogeogr.
539 Palaeoclimatol. Palaeoecol. 460, 35–49. https://doi.org/10.1016/J.PALAEO.2016.07.026
540 Hancy, A.D. and Antcliffe, J.B., 2020. Anoxia can increase the rate of decay for cnidarian
541 tissue: Using *Actinia equina* to understand the early fossil record. Geobiology, 18(2),

542 167-184.
543 Harper, D.A. and Servais, T., 2018. Contextualizing the onset of the Great Ordovician
544 Biodiversification Event. Lethaia 51(2), 149-150.
545 Hoda, K., Bowlus, C.L., Chu, T.W., Gruen, J.R., 2013. Iron metabolism and related disorders.
546 Emery Rimoin's Princ. Pract. Med. Genet. 1–41. https://doi.org/10.1016/B978-0-12-
547 383834-6.00106-3
548 Hou, X., Siveter, David J., Siveter, Derek J., Aldridge, R.J., Cong, P., Gabbott, S.E., Ma, X.,
549 Purnell, M.A., Williams, M., 2004. The Cambrian fossils of Chengjiang, China : the
550 flowering of early animal life. Blackwell.
551 Kouketsu, Y., Mizukami, T., Mori, H., Endo, S., Aoya, M., Hara, H., Nakamura, D., Wallis,
552 S., 2014. A new approach to develop the Raman carbonaceous material geothermometer
553 for low-grade metamorphism using peak width. Isl. Arc 23, 33–50.
554 https://doi.org/10.1111/iar.12057
555 Kouraiss, K., El Hariri, K., El Albani, A., Azizi, A., Mazurier, A., Lefebvre, B., 2019.
556 Digitization of fossils from the Fezouata Biota (Lower Ordovician, Morocco):
557 Evaluating computed tomography and photogrammetry in collection enhancement.
558 Geoheritage 11, 1889–1901. https://doi.org/10.1007/s12371-019-00403-z
559 Lamsdell, J.C., Hoşgör, İ., Selden, P.A., 2013. A new Ordovician eurypterid (Arthropoda:
560 Chelicerata) from southeast Turkey: Evidence for a cryptic Ordovician record of
561 Eurypterida. Gondwana Res. 23, 354–366. https://doi.org/10.1016/J.GR.2012.04.006
562 Larsen, F., Postma, D., 1997. Nickel mobilization in a groundwater well field: release by
563 pyrite oxidation and desorption from manganese oxides. Environ. Sci. Technol. 31,
564 2589–2595. https://doi.org/10.1021/ES9610794
565 Lefebvre, B., El Hariri, K., Lerosey-Aubril, R., Servais, T., Van Roy, P., 2016a. The Fezouata
566 Shale (Lower Ordovician, Anti-Atlas, Morocco): a historical review. Palaeogeogr.

Palaeoclimatol. Palaeoecol, 460, 7–23.

Lefebvre, B., Allaire, N., Guensburg, T.E., Hunter, A.W., Kouraïss, K., Martin, E.L.O., Nardin, E., Noailles, F., Pittet, B., Sumrall, C.D., Zamora, S., Lefebvre, B., Allaire, N., Guensburg, T.E., Hunter, A.W., Kouraïss, K., Martin, E.L.O., Nardin, E., Noailles, F., Pittet, B., Sumrall, C.D., Zamora, S., 2016b. Palaeoecological aspects of the diversification of echinoderms in the Lower Ordovician of central Anti-Atlas, Morocco. Palaeogeogr. Palaeoclimatol. Palaeoecol. 460, 97–121. https://doi.org/10.1016/J.PALAEO.2016.02.039

Lefebvre, B., Gutiérrez-Marco, J.C., Lehnert, O., Martin, E.L.O., Nowak, H., Akodad, M., El Hariri, K., Servais, T., 2018. Age calibration of the Lower Ordovician Fezouata *Lagerstätte*, Morocco. Lethaia 51, 296–311. https://doi.org/10.1111/let.12240

Lefebvre, B., Guensburg, T.E., Martin, E.L.O., Mooi, R., Nardin, E., Nohejlová, M., Saleh, F., Kouraïss, K., El Hariri, K., David, B., 2019. Exceptionally preserved soft parts in fossils from the Lower Ordovician of Morocco clarify stylophoran affinities within basal deuterostomes. Geobios 52, 27–36. https://doi.org/10.1016/J.GEOBIOS.2018.11.001

Lehnert, O., Nowak, H., Sarmiento, G.N., Gutiérrez-Marco, J.C., Akodad, M., Servais, T., 2016. Conodonts from the Lower Ordovician of Morocco—Contributions to age and faunal diversity of the Fezouata *Lagerstätte* and peri-Gondwana biogeography. Palaeogeogr. Palaeoclimatol. Palaeoecol. 460, 50–61.

Lei, Q.-P., Han, J., Ou, Q., Wan, X.-Q., 2014. Sedentary habits of Anthozoa-like animals in the Chengjiang *Lagerstätte*: Adaptive strategies for Phanerozoic-style soft substrates. Gondwana Res. 25, 966–974. https://doi.org/10.1016/J.GR.2013.01.007

Lerosey-Aubril, R., Paterson, J.R., Gibb, S., Chatterton, B.D.E., 2017. Exceptionally-preserved late Cambrian fossils from the McKay Group (British Columbia, Canada) and the evolution of tagmosis in aglaspidid arthropods. Gondwana Res. 42, 264–279.

592 https://doi.org/10.1016/J.GR.2016.10.013
593 Li, Y.-L., Vali, H., Yang, J., Phelps, T.J., Zhang, C.L., 2006. Reduction of iron oxides
594 enhanced by a sulfate-reducing bacterium and biogenic H2S. Geomicrobiol. J. 23, 103–
595 117. https://doi.org/10.1080/01490450500533965
596 Liu, J., Shu, D., Han, J., Zhang, Z., Zhang, X., 2008. Origin, diversification, and relationships
597 of Cambrian lobopods. Gondwana Res. 14, 277–283.
598 https://doi.org/10.1016/J.GR.2007.10.001
599 Ma, X., Hou, X., Edgecombe, G.D., Strausfeld, N.J., 2012. Complex brain and optic lobes in
600 an early Cambrian arthropod. Nature 490, 258–261. https://doi.org/10.1038/nature11495
601 Ma, X., Cong, P., Hou, X., Edgecombe, G.D., Strausfeld, N.J., 2014. An exceptionally
602 preserved arthropod cardiovascular system from the early Cambrian. Nat. Commun. 5,
603 3560. https://doi.org/10.1038/ncomms4560
604 Ma, X., Edgecombe, G.D., Hou, X., Goral, T., Strausfeld, N.J., 2015. Preservational pathways
605 of corresponding brains of a Cambrian euarthropod. Curr. Biol. 25, 2969–2975.
606 https://doi.org/10.1016/j.cub.2015.09.063
607 Marante, A., 2008. Architecture et dynamique des systèmes sédimentaires silico-clastiques
608 sur la plate-forme géante nord-gondwanienne. Université Michel Montaigne, Bordeaux
609 3. Unpublished.
610 Martin, E., 2016. Communautés animales du début de l'Ordovicien (env. 480 Ma): études
611 qualitatives et quantitatives à partir des sites à préservation exceptionnelle des Fezouata,
612 Maroc. Unpubl. PhD thesis, Université Lyon 1. p.483.
613 Martin, E., Lefebvre, B., Vaucher, R., 2015. Taphonomy of a stylophoran-dominated
614 assemblage in the Lower Ordovician of Zagora area (centrak Anti-Atlas, Morocco). In:
615 Zamora, S., Rabano, I. (Eds.), Progress in Echinoderm Palaeobiology. Cuadernos Mus.
616 Geomin. 19, pp. 95-100.

617 Martin, E.L.O., Pittet, B., Gutiérrez-Marco, J.-C., Vannier, J., El Hariri, K., Lerosey-Aubril,
618 R., Masrour, M., Nowak, H., Servais, T., Vandenbroucke, T.R.A., Van Roy, P., Vaucher,
619 R., Lefebvre, B., 2016a. The Lower Ordovician Fezouata Konservat-Lagerstätte from
620 Morocco: Age, environment and evolutionary perspectives. Gondwana Res. 34, 274–
621 283. https://doi.org/10.1016/J.GR.2015.03.009
622 Martin, E.L.O., Vidal, M., Vizcaïno, D., Vaucher, R., Sansjofre, P., Destombes, J., 2016b.
623 Biostratigraphic and palaeoenvironmental controls on the trilobite associations from the
624 Lower Ordovician Fezouata Shale of the central Anti-Atlas, Morocco. Palaeogeogr.
625 Palaeoclimatol. Palaeoecol. 460, 142–154.
626 https://doi.org/10.1016/J.PALAEO.2016.06.003
627 Mazzetti, L., Thistlethwaite, P.J., 2002. Raman spectra and thermal transformations of
628 ferrihydrite and schwertmannite. J. Raman Spectrosc. 33, 104–111.
629 https://doi.org/10.1002/jrs.830
630 McMahon, S., Anderson, R.P., Saupe, E.E., Briggs, D.E.G., 2016. Experimental evidence that
631 clay inhibits bacterial decomposers: Implications for preservation of organic fossils.
632 Geology 44, 867–870. https://doi.org/10.1130/G38454.1
633 Moysiuk, J., Smith, M.R., Caron, J.-B., 2017. Hyoliths are Palaeozoic lophophorates. Nature
634 541, 394–397. https://doi.org/10.1038/nature20804
635 Moysiuk, J., Caron, J.-B., 2019. A new hurdiid radiodont from the Burgess Shale evinces the
636 exploitation of Cambrian infaunal food sources. Proc. R. Soc. B Biol. Sci. 286,
637 20191079. https://doi.org/10.1098/rspb.2019.1079
638 Na, L. and Kiessling, W., 2015. Diversity partitioning during the Cambrian radiation.
639 Proceedings of the National Academy of Sciences 112(15), 4702-4706.
640 Nanglu, K., Caron, J.B., Gaines, R, 2020. The Burgess Shale paleocommunity with new
641 insights from Marble Canyon , British Columbia. Paleobiology 46, 58–81.

642 Nowak, H., Pittet, B., Vaucher, R., Akodad, M., Gaines, R.R., Vandenbroucke, T.R.A., 2016.
643 Palynomorphs of the Fezouata Shale (Lower Ordovician, Morocco): Age and
644 environmental constraints of the Fezouata Biota. Palaeogeogr. Palaeoclimatol.
645 Palaeoecol. 460, 62–74. https://doi.org/10.1016/J.PALAEO.2016.03.007
646 Parry, L.A., Smithwick, F., Nordén, K.K., Saitta, E.T., Lozano-Fernandez, J., Tanner, A.R.,
647 Caron, J.-B., Edgecombe, G.D., Briggs, D.E.G., Vinther, J., 2018. Soft-bodied fossils are
648 not simply rotten carcasses - Toward a holistic understanding of exceptional fossil
649 preservation. BioEssays 40, 1700167. https://doi.org/10.1002/bies.201700167
650 Pérez-Peris, F., Laibl, L., Lustri, L., Gueriau, P., Antcliffe, J.B., Bath Enright O.G., Daley,
651 A.C., in press. A new nektaspidid euarthropod from the Lower Ordovician of Morocco.
652 Geological Magazine.
653 Potter, R.M., Rossman, G.R., 1979. The manganese- and iron-oxide mineralogy of desert
654 varnish. Chem. Geol. 25, 79–94. https://doi.org/10.1016/0009-2541(79)90085-8
655 Purnell, M.A., Donoghue, P.J.C., Gabbott, S.E., McNamara, M.E., Murdock, D.J.E., Sansom,
656 R.S., 2018. Experimental analysis of soft-tissue fossilization: opening the black box.
657 Palaeontology 61, 317–323. https://doi.org/10.1111/pala.12360
658 Rahl, J.M., Anderson, K.M., Brandon, M.T., Fassoulas, C., 2005. Raman spectroscopic
659 carbonaceous material thermometry of low-grade metamorphic rocks: Calibration and
660 application to tectonic exhumation in Crete, Greece. Earth Planet. Sci. Lett. 240, 339–
661 354. https://doi.org/10.1016/J.EPSL.2005.09.055
662 Raiswell, R., Whaler, K., Dean, S., Coleman, M.., Briggs, D.E.., 1993. A simple three-
663 dimensional model of diffusion-with-precipitation applied to localised pyrite formation
664 in framboids, fossils and detrital iron minerals. Mar. Geol. 113, 89–100.
665 https://doi.org/10.1016/0025-3227(93)90151-K
666 Raiswell, R., Newton, R., Bottrell, S.H., Coburn, P.M., Briggs, D.E., Bond, D.P., Poulton,

667 S.W., 2008. Turbidite depositional influences on the diagenesis of Beecher's Trilobite
668 Bed and the Hunsrück Slate; sites of soft tissue pyritization. Am. J. Sci. 308, 105–129.
669 Rasmussen, C.M., Kröger, B., Nielsen, M.L. and Colmenar, J., 2019. Cascading trend of
670 Early Paleozoic marine radiations paused by Late Ordovician extinctions. Proceedings of
671 the National Academy of Sciences 116(15), 7207-7213.
672 Saleh, F., Candela, Y., Harper, D.A.T., Polechovà, M., Pittet, B., Lefebvre, B., 2018. Storm-
673 induced community dynamics in the Fezouata Biota (Lower Ordovician, Morocco).
674 Palaios 33, 535–541.
675 Saleh, F., Pittet, B., Perrillat, J., Lefebvre, B., 2019. Orbital control on exceptional fossil
676 preservation. Geology 47, 1–5. https://doi.org/10.1130/G45598.1
677 Saleh, F., Pittet, B., Sansjofre, P., Guériau, P., Lalonde, S., Perrillat, J.-P., Vidal, M., Lucas,
678 V., EL Hariri, K., Kouraïss, K., Lefebvre, B., 2020a. Taphonomic pathway of
679 exceptionally preserved fossils in the Lower Ordovician of Morocco. Geobios 60.
680 https://doi.org/10.1016/j.geobios.2020.04.001
681 Saleh, F, Vidal, M., Laibl, L., Sansjofre, P., Gueriau, P., Perez Peris, F., Lustri, L., Lucas, V.,
682 Lefebvre, B., Pittet, B., El Hariri, K., Daley, A.C., 2020b. Large trilobites in a stress-free
683 Early Ordovician environment. Geol. Mag. https://doi.org/10.1017/S0016756820000448
684 Saleh, F. Daley, A.C., Lefebvre, B., Pittet, B., Perrillat, J.P., 2020c. Biogenic iron preserves
685 structures during fossilization: A hypothesis. BioEssays 42.
686 https://doi.org/10.1002/bies.201900243
687 Saleh, F., Antcliffe, J.B., Lefebvre, B., Pittet, B., Laibl, L., Perez Peris, F., Lustri, L., Gueriau,
688 P., Daley, A.C., 2020d. Taphonomic bias in exceptionally preserved biotas. Earth Planet.
689 Sci. Lett. 529. https://doi.org/10.1016/j.epsl.2019.115873
690 Sansom, R.S., Gabbott, S.E., Purnell, M.A., 2010. Non-random decay of chordate characters
691 causes bias in fossil interpretation. Nature 463, 797–800.

https://doi.org/10.1038/nature08745

Schiffbauer, J.D., Xiao, S., Cai, Y., Wallace, A.F., Hua, H., Hunter, J., Xu, H., Peng, Y., Kaufman, A.J., 2014. A unifying model for Neoproterozoic–Palaeozoic exceptional fossil preservation through pyritization and carbonaceous compression. Nat. Commun. 5, 5754. https://doi.org/10.1038/ncomms6754

Servais, T., Cascales-Miñana, B., Cleal, C.J., Gerrienne, P., Harper, D.A. and Neumann, M., 2019. Revisiting the Great Ordovician Diversification of land plants: Recent data and perspectives. Palaeogeogr., Palaeoclimatol., Palaeoecol. 534, 109280.

Smith, M.R., Caron, J.-B., 2010. Primitive soft-bodied cephalopods from the Cambrian. Nature 465, 469–472.

Stigall, A.L., Edwards, C.T., Freeman, R.L. and Rasmussen, C.M., 2019. Coordinated biotic and abiotic change during the Great Ordovician Biodiversification Event: Darriwilian assembly of early Paleozoic building blocks. Palaeogeogr., Palaeoclimatol., Palaeoecol. 530, 249-270.

Tanaka, G., Hou, X., Ma, X., Edgecombe, G.D., Strausfeld, N.J., 2013. Chelicerate neural ground pattern in a Cambrian great appendage arthropod. Nature 502, 364–367. https://doi.org/10.1038/nature12520

Topper, T.P., Greco, F., Hofmann, A., Beeby, A., Harper, D.A.T., 2018. Characterization of kerogenous films and taphonomic modes of the Sirius Passet *Lagerstätte*, Greenland. Geology 46, 359–362. https://doi.org/10.1130/G39930.1

Torsvik, T., Cocks, L., 2011. The Palaeozoic palaeogeography of central Gondwana. Geol. Soc. London, Spec. 357, 137–166.

Torsvik, T., Cocks, L., 2013. New global palaeogeographical reconstructions for the Early Palaeozoic and their generation. Geol. Soc. London, Mem. 38, 5–24.

Van Roy, P., Orr, P.J., Botting, J.P., Muir, L.A., Vinther, J., Lefebvre, B., El Hariri, K.,

717 Briggs, D.E.G., 2010. Ordovician faunas of Burgess Shale type. Nature 465, 215–218.
718 https://doi.org/10.1038/nature09038
719 Van Roy, P., Briggs, D.E. and Gaines, R.R., 2015a. The Fezouata fossils of Morocco; an
720 extraordinary record of marine life in the Early Ordovician. Journal of the Geological
721 Society 172(5), 541-549.
722 Van Roy, P., Daley, A.C., Briggs, D.E.G., 2015b. Anomalocaridid trunk limb homology
723 revealed by a giant filter-feeder with paired flaps. Nature 522, 77–80.
724 https://doi.org/10.1038/nature14256
725 Vannier, J., Vidal, M., Marchant, R., El Hariri, K., Kouraïss, K., Pittet, B., El Albani, A.,
726 Mazurier, A., Martin, E.L.., 2019. Collective behaviour in 480-million-year-old trilobite
727 arthropods from Morocco. Sci. Rep. 9.
728 Vaucher, R., Martin, E.L.O., Hormière, H., Pittet, B., 2016. A genetic link between
729 Konzentrat- and Konservat-*Lagerstätten* in the Fezouata Shale (Lower Ordovician,
730 Morocco). Palaeogeogr. Palaeoclimatol. Palaeoecol. 460, 24–34.
731 https://doi.org/10.1016/J.PALAEO.2016.05.020
732 Vaucher, R., Pittet, B., Hormière, H., Martin, E.L.O., Lefebvre, B., 2017. A wave-dominated,
733 tide-modulated model for the Lower Ordovician of the Anti-Atlas, Morocco.
734 Sedimentology 64, 777–807. https://doi.org/10.1111/sed.12327
735 Vinther, J., Van Roy, P., Briggs, D.E.G., 2008. Machaeridians are Palaeozoic armoured
736 annelids. Nature 451, 185–188. https://doi.org/10.1038/nature06474
737 Vinther, J., Parry, L., Briggs, D.E.G., Van Roy, P., 2017. Ancestral morphology of crown-
738 group molluscs revealed by a new Ordovician stem aculiferan. Nature 542, 471–474.
739 https://doi.org/10.1038/nature21055
740 Warner, N., Lgourna, Z., Bouchaou, L., Boutaleb, S., Tagma, T., Hsaissoune, M., Vengosh,
741 A., 2013. Integration of geochemical and isotopic tracers for elucidating water sources

and salinization of shallow aquifers in the sub-Saharan Drâa Basin, Morocco. Appl. Geochemistry 34, 140–151. https://doi.org/10.1016/J.APGEOCHEM.2013.03.005

Zhang, X., Liu, W., Zhao, Y., 2008. Cambrian Burgess Shale-type *Lagerstätten* in South China: Distribution and significance. Gondwana Res. 14, 255–262.

Figure captions

Figure 1. Fossils from the Fezouata Biota. (A) The distribution of classes among fossiliferous levels from the Fezouata Shale. (B) Xiphosuran chelicerate indet. AA.TER.OI.3, (C) hyolith with preserved internal parts YPM515750, (D) *Bavarilla* sp., trilobite with preserved antennae AA.BIZ15.OI.16, (E) *Furca*, marrellomorph arthropod AA.BIZ31.OI.39, (F) *Palaeoscolex*? *tenensis*, palaeoscolecid worm, AA.BGF2.OI.1, (G) Aglaspidid arthropod, AA-TER-OI-5, (H) *Pirania auraeum*, demosponge AA.JBZ.OI.115, (I) *Thelxiope*-like arthropod YPM 226544, (J) *Taricciocia tazagurtensis*, liwiid arthropod, MGL102155a, (K) *Bohemiaecystis* sp., stylophoran echinoderm with preserved soft tissues including the water vascular system AA.BIZ15.OI.259, (L) frontal appendages of *Aegirocassis benmoulae*, radiodont arthropod YPM 527123. AA: University Cadi-Ayyad, Marrakesh, YPM: Yale Peabody Museum, MGL: Lausanne University.

Figure 2. Processes and pathways involved during the transfer of organic matter from the biosphere into the lithosphere (i.e. fossilization). These processes determine which characters from the original morphology are lost or retained (Sansom et al., 2010; Bath Enright, 2018; Parry et al., 2018; Purnell et al., 2018).

Figure 3. Ordovician lithostratigraphic sequencing of the Zagora area (modified from Marante, 2008) completed with graptolite biostratigraphy for the Fezouata Shale (based on Gutiérrez-Marco and Martin, 2016). Exceptionally preserved fossils occur discontinuously (every

766 100,000 years) within eccentricity-controlled levels belonging to two stratigraphic intervals
767 (Saleh et al., 2019).

768 **Figure 4.** Sedimentary structures in the Fezouata Shale, typical of a storm-wave dominated
769 environment. (A) Storm bed surrounded by background sediments, (B) bed surface displaying
770 2D oscillatory ripples of centimetric wavelength, (C) storm beds displaying a normal grading,
771 (D) hummocky cross-stratified sandstone showing a metric wavelength, (E) In shallower
772 settings, a tidal modulation of storm waves occurs and is recorded as a repeated stack of larger
773 (low tide) to smaller (high tide) oscillatory structures within fine-grained sandstone, (F) In distal
774 settings, fossils were decaying on the seafloor prior to their burial by storm-induced deposits.
775 Disarticulated skeletal elements of the rhombiferan echinoderm *Macrocystella bohemica* in
776 green, trilobites in blue, bioturbations in pink, and undetermined elements in beige, (G) most
777 exceptionally preserved BST fossils are preserved *in-situ* under storm-induced beds. Some
778 shelly organisms can be preserved within background sediments because they are resistant to
779 decay and they do not require an event deposition (Kouraiss et al., 2019; Vannier et al., 2019;
780 Saleh et al., 2020a).

781 **Figure 5.** Body size variations of epibenthic, shallow endobenthic, and deep endobenthic taxa
782 along the proximal-distal axis of the Fezouata Shale accordingly with differences in burial rates
783 and oxygenation (OMZ= Oxygen Minimum Zone; SWB: Storm Wave Base).

784 **Figure 6.** Different scenarios of decay and mineralization according to a model based on Fe
785 availability in biological tissues, Fe reactivity in the sediments and H_2S production (Saleh et
786 al., 2020c). (A) Absence of pyrite precipitation due to a delay in burial (*Platypeltoides*
787 *magrebiensis* trilobite; AA.TGR0a.OI.132). (B, C) Most of the organism is pyritized including
788 the body wall (*Triarthrus eatoni* trilobite; YPM.516160) (Farrell et al., 2011). (D) Pyritized
789 parts of the digestive system (*Megistaspis hammondi* trilobite*;* MGM.6755X) (Gutiérrez-Marco
790 et al., 2017). (E) Pyritized nervous system preserved as a dark brown/black imprint (*Fuxanhuia*

protensa arthropod; YKLP.15006) (Ma et al., 2015). The purple spectrum is indicative of chamosite/berthierine identified using X-Ray Diffraction. The red arrows and boxes are examples of pyritized areas identified using Raman Spectroscopy and Backscattered Electronic Microscopy on fossils and fresh sediments. Orange boxes are examples of carbonaceous preservation identified under Raman Spectroscopy and Backscattered Electronic Microscopy as well. MGM: Museo Geominero, Madrid, YKLP: Yunnan Key Laboratory for Paleobiology.

Figure 7. Modern weathering effect on fossils from the Fezouata Shale. Manganese oxides start the oxidation process (A) followed by dissolved oxygen in pore waters (B). The resulting products of these reactions are respectively manganese sulfates (B) and sulfuric acid (C). Sulfuric acid leaches calcium from the skeletal elements of the fossils (D). If extensive weathering occurs, all C is leached from fossils and replaced by modern, star shaped iron oxides from circulating water (E). This process explains the absence of Ca in the skeleton of a solutan echinoderm (CASG72938) and the enrichment in Mn- deposits surrounding the extensively weathered marrellomorph (AA.BIZ31.OI.39). Modern star-shaped iron oxides that are deposited during this process gave the extensively weathered marrellomorph a red/orange color in comparison to the less weathered marrellomorph (AA.BIZ15.OI.364). CASG: California Academy of Sciences.

Figure 8. (A) *Branchiocaris pretiosa*, a crustacean arthropod from the Burgess Shale USNM189028nc preserving three types of biological structures. (B) Differences in the preservational pattern between the Fezouata Shale and the Burgess Shale and the Chengjiang Biota (Saleh et al., 2020d). (C) Exceptionally preserved biotas during the Cambrian and Ordovician plotted on the global diversity curve from Rasmussen et al. (2019). Note that the Fezouata Shale does not preserve completely cellular organisms such as cambroernids and chordates; Cambrian Explosion (CE), Ordovician Radiation (OR). USNM: United States National Museum of Natural history.

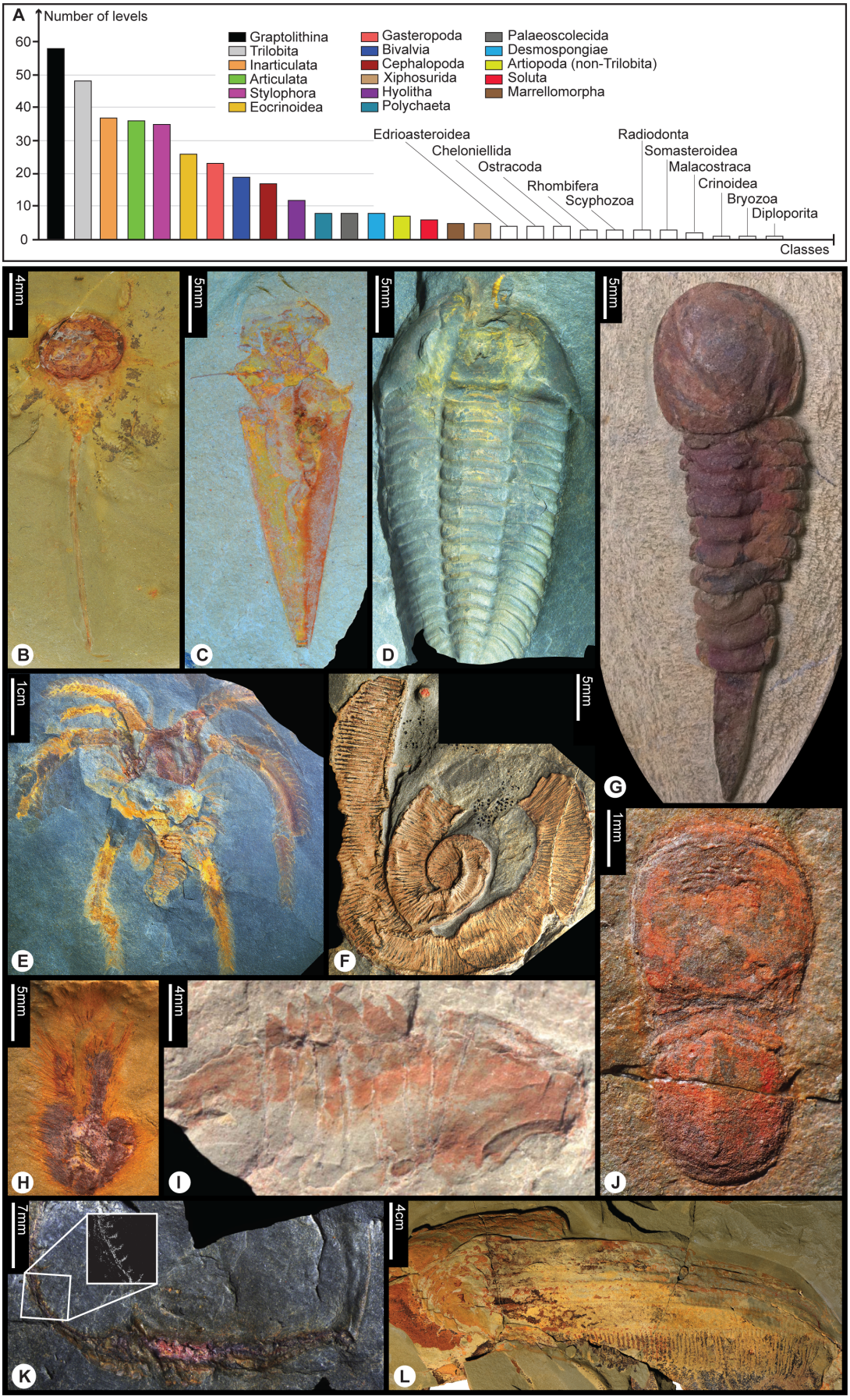
A
Number of levels
60
50
40
30
20
10
0
Graptolithina
Trilobita
Inarticulata
Articulata
Stylophora
Eocrinoidea
Gasteropoda
Bivalvia
Cephalopoda
Xiphosurida
Hyolitha
Polychaeta
Palaeoscolecida
Desmospongiae
Artiopoda (non-Trilobita)
Soluta
Marrellomorpha
Edrioasteroidea
Cheloniellida
Ostracoda
Rhombifera
Scyphozoa
Radiodonta
Somasteroidea
Malacostraca
Crinoidea
Bryozoa
Diploporita
Classes
4mm
B
5mm
C
5mm
D
5mm
G
1cm
E
5mm
F
1mm
J
5mm
H
4mm
I
7mm
K
4cm
L

Figure 1

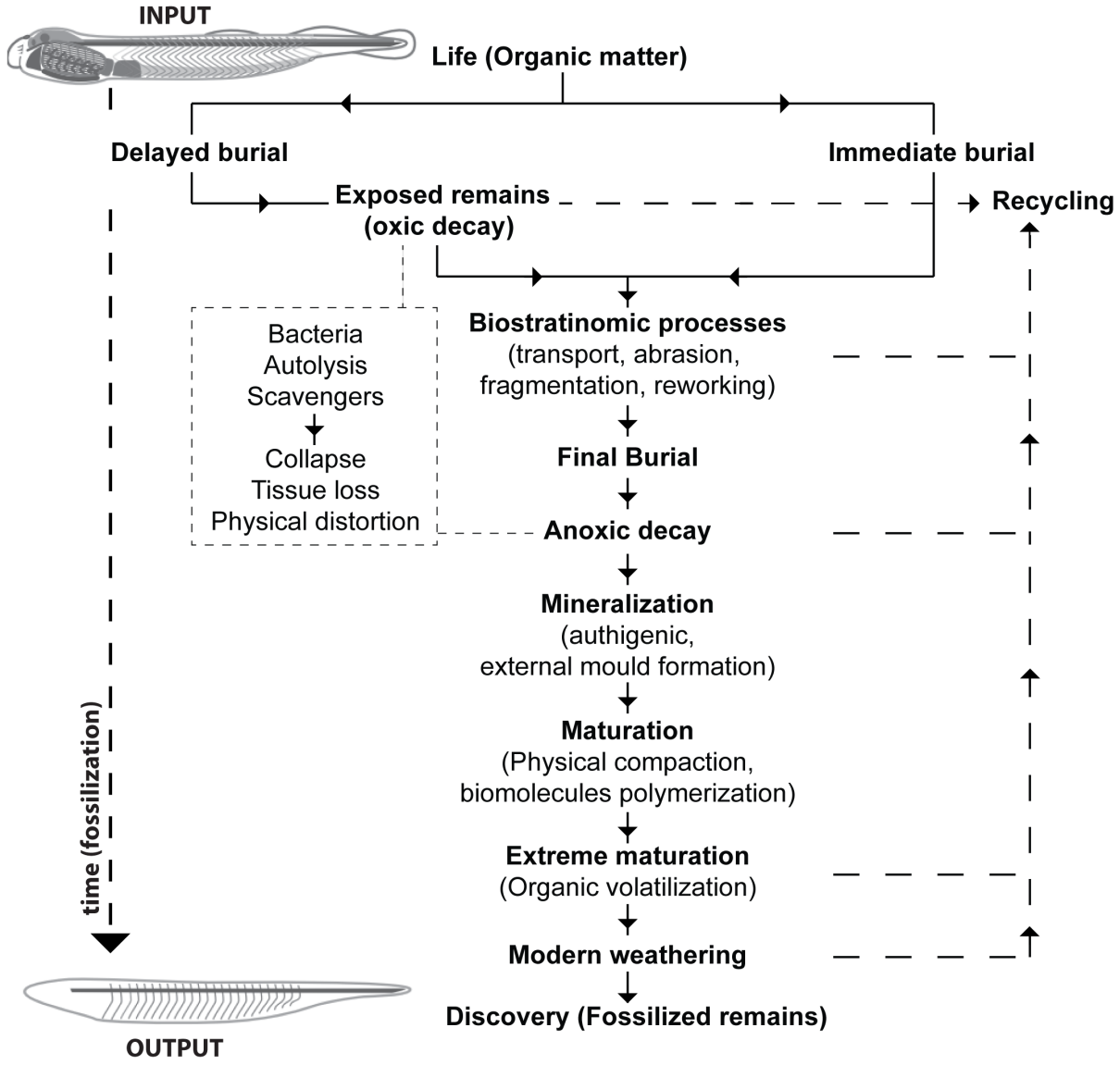

818

819 **Figure 2**

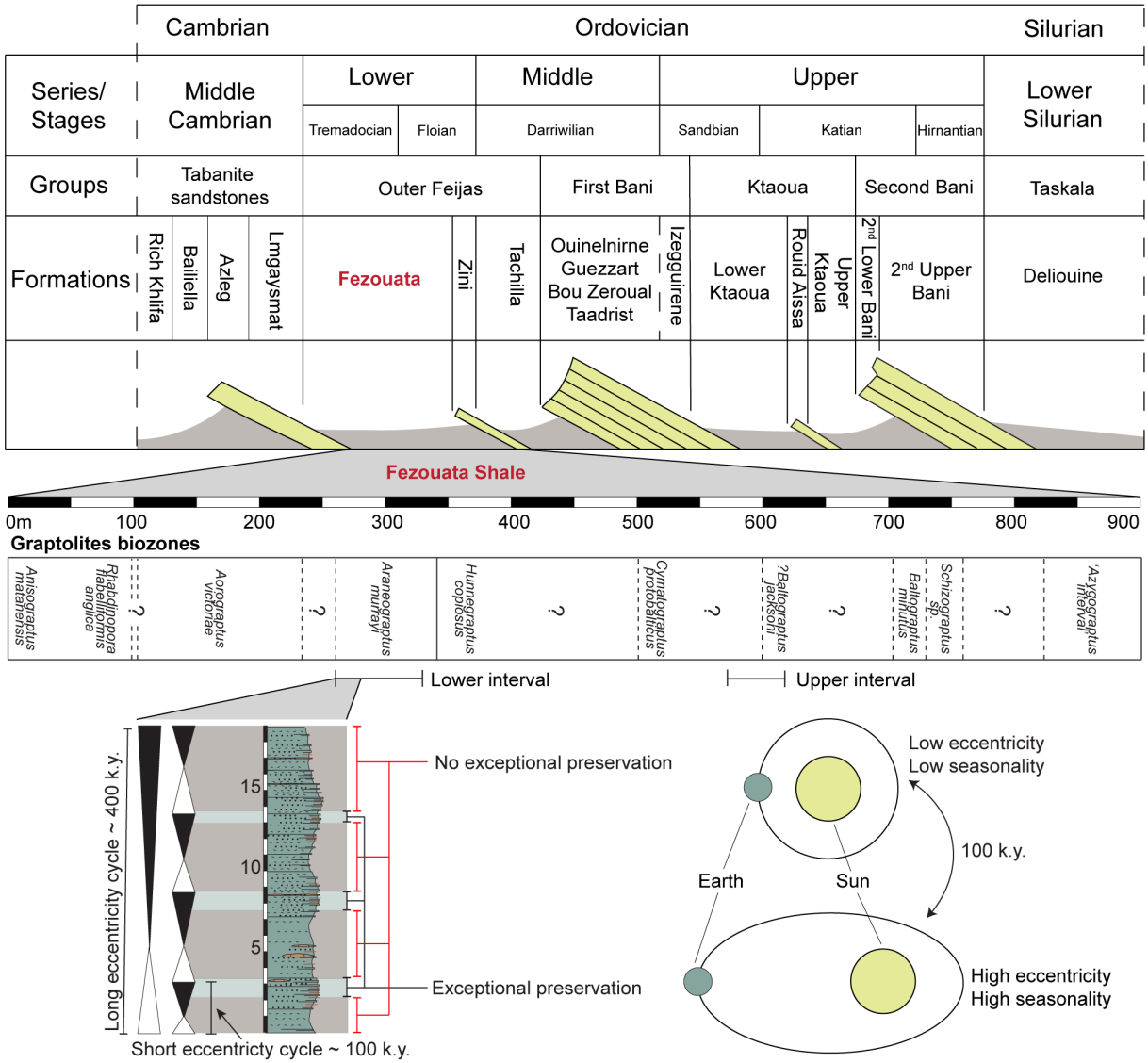

820

821 **Figure 3**

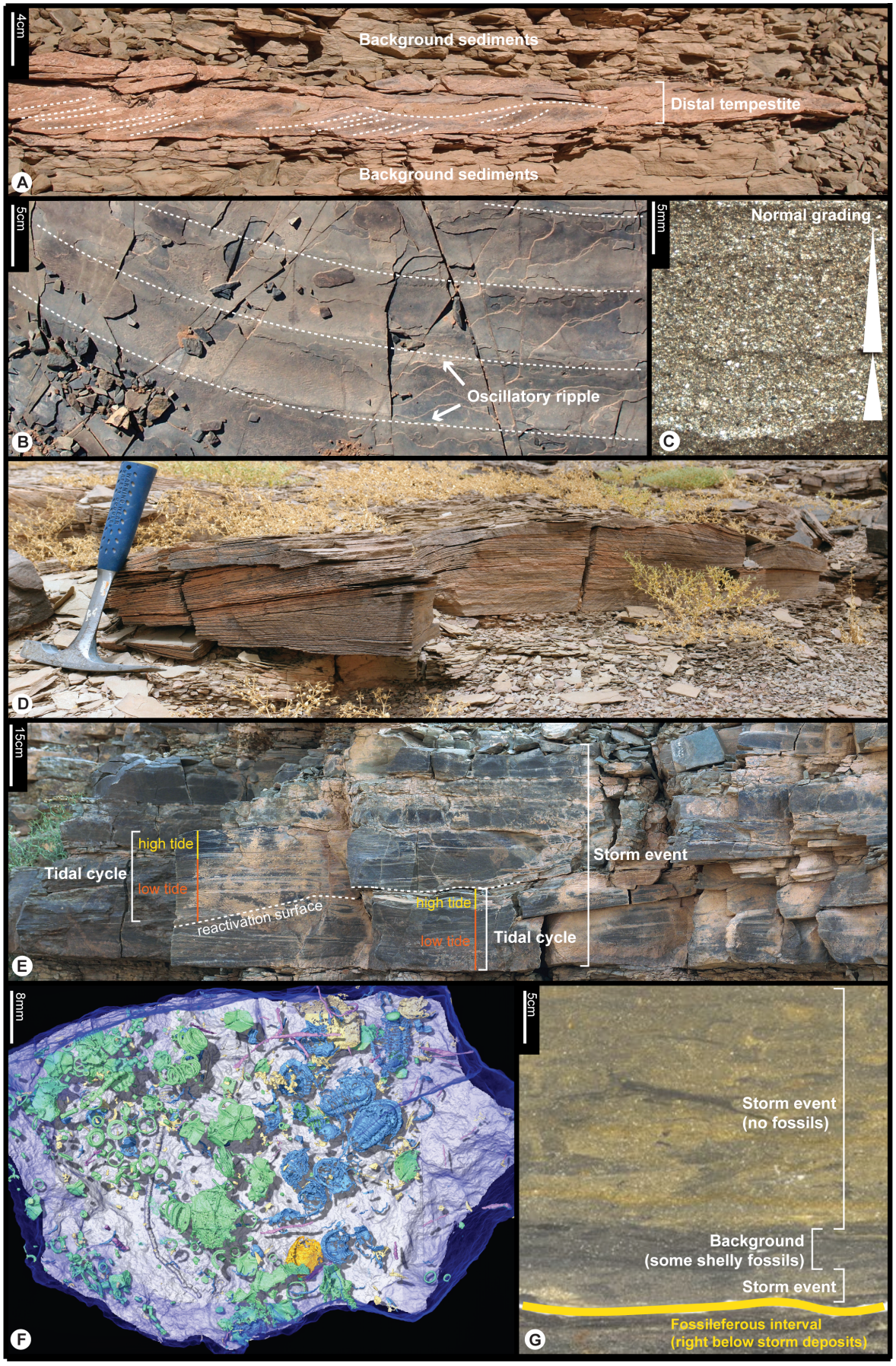

822

823 **Figure 4**

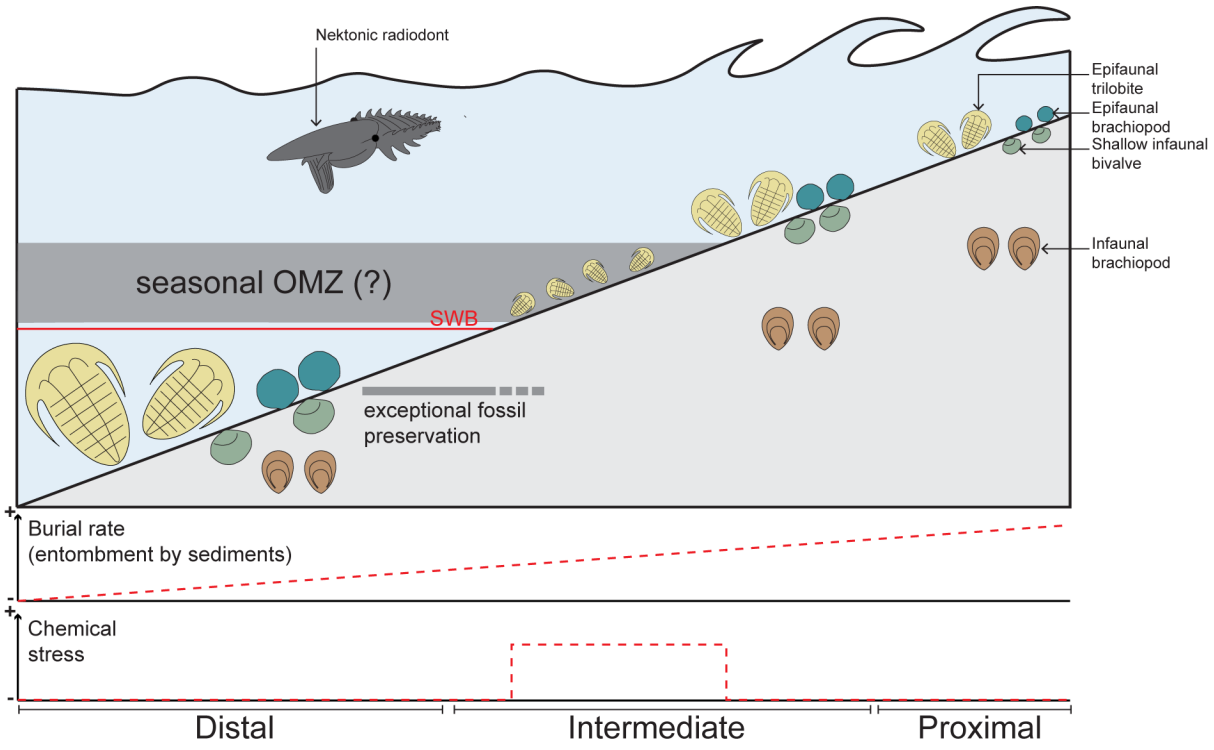

824

825 **Figure 5**

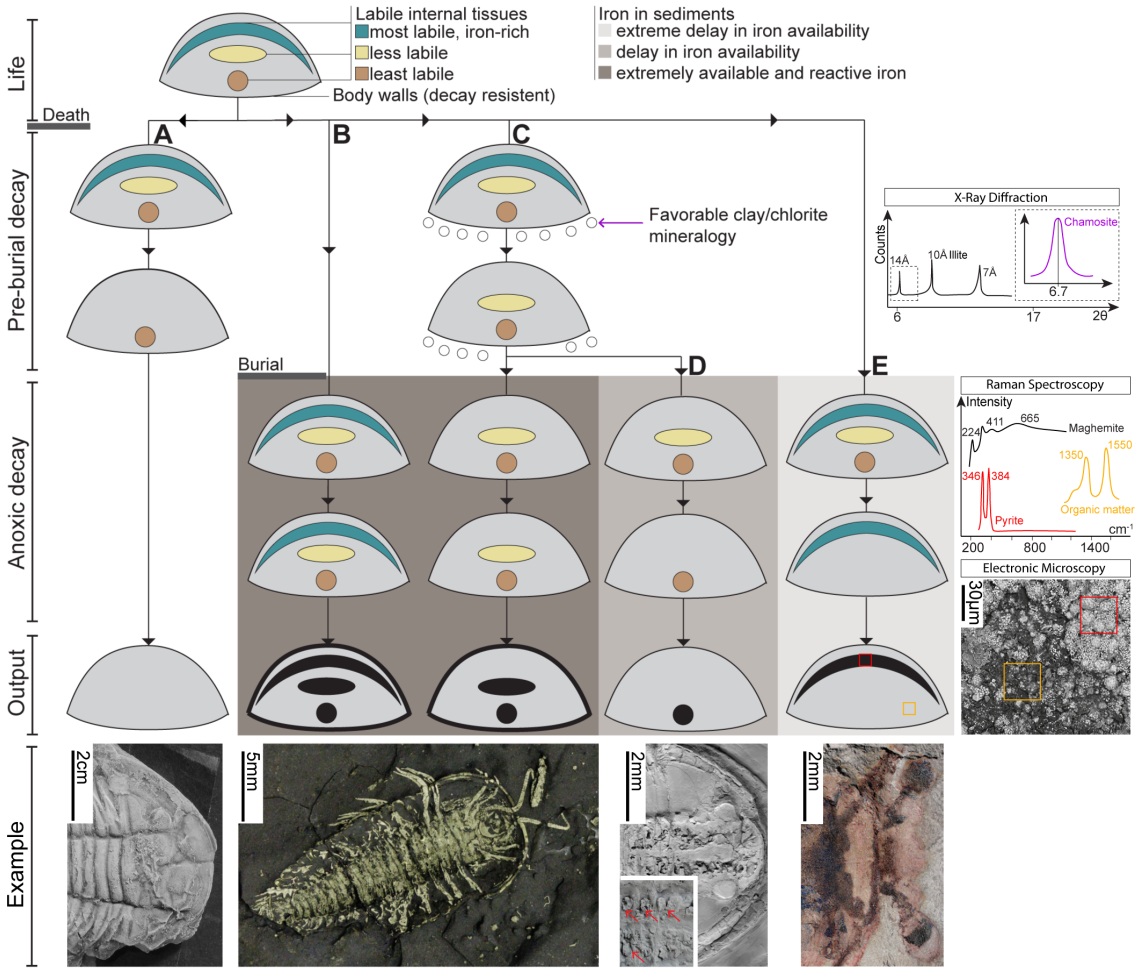

826

827 **Figure 6**

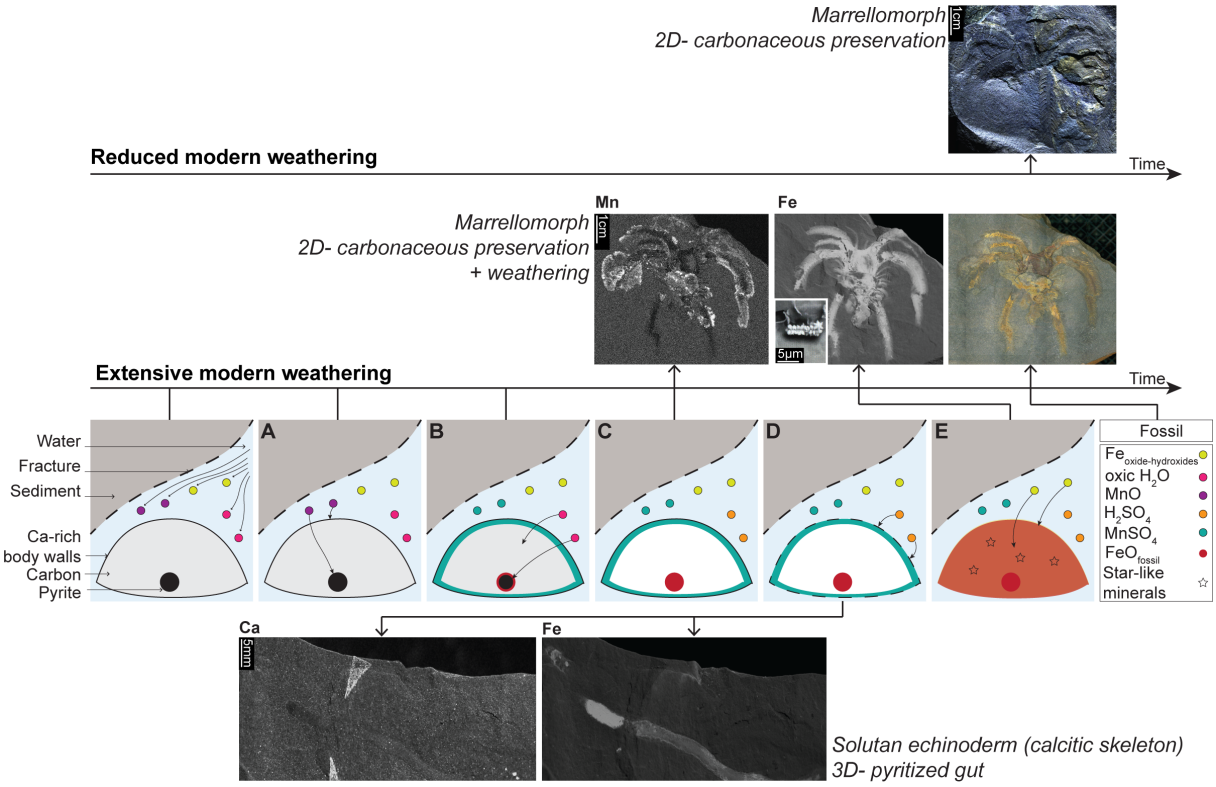

828

829 **Figure 7**

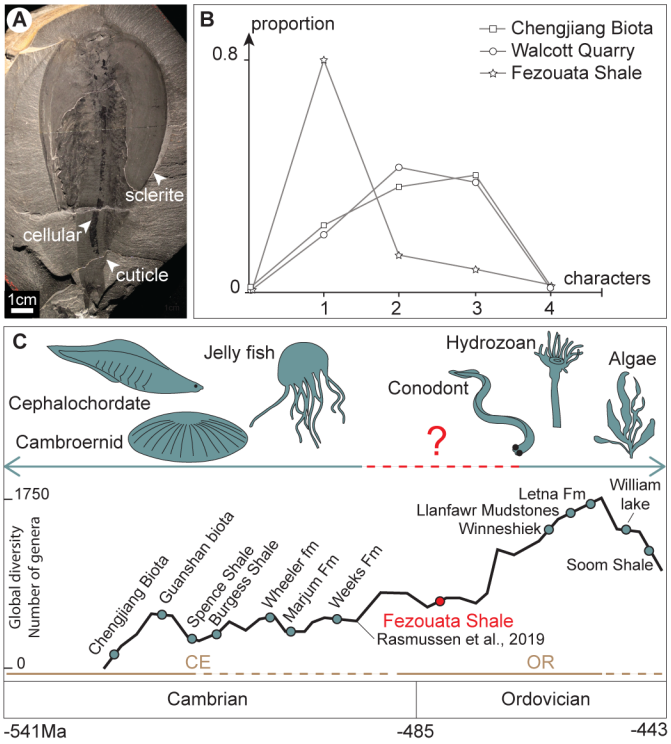
A
sclerite
cellular
cuticle
1cm
B
proportion
0.8
0
1
2
3
4
characters
Chengjiang Biota
Walcott Quarry
Fezouata Shale
C
Jelly fish
Cephalochordate
Cambroernid
Hydrozoan
Conodont
Algae
?
1750
Global diversity
Number of genera
0
Chengjiang Biota
Guanshan biota
Spence Shale
Burgess Shale
Wheeler fm
Marjum Fm
Weeks Fm
Fezouata Shale
Rasmussen et al., 2019
Letna Fm
Llanfawr Mudstones
Winneshiek
William lake
Soom Shale
CE
OR
Cambrian
Ordovician
-541Ma
-485
-443

Figure 8